Planta (2007) 226:917–927
DOI 10.1007/s00425-007-0538-7

ORIGINAL ARTICLE

Patterns of asexual reproduction in *Nannochloris bacillaris* and *Marvania geminata* (Chlorophyta, Trebouxiophyceae)

Maki Yamamoto · Toshikazu Nishikawa · Hiroyuki Kajitani · Shigeyuki Kawano

Received: 22 February 2007 / Accepted: 23 April 2007 / Published online: 23 May 2007

Abstract Non-flagellated vegetative green algae of the Trebouxiophyceae propagate mainly by autosporulation. In this manner, the mother cell wall is shed following division of the protoplast in each round of cell division. Binary fission type *Nannochloris* and budding type *Marvania* are also included in the Trebouxiophyceae. Phylogenetic trees based on the actin sequences of Trebouxiophyceae members revealed that the binary fission type *Nannochloris bacillaris* and the budding type *Marvania geminata* are closely related in a distal monophyletic group. Our results suggest that autosporulation is the ancestral mode of cell division in Trebouxiophyceae. To elucidate how non-autosporulative mechanisms such as binary fission and budding evolved, we focused on the cleavage of the mother cell wall. Cell wall development was analyzed using a cell wall-specific fluorescent dye, Fluostain I. Exfoliation of the mother cell wall was not observed in either *N. bacillaris* or *M. geminata*. We then compared the two algae by transmission electron microscopy with rapid freeze fixation and freeze substitution; in both algae, the mother cell wall was cleaved at the site of cell division, but remained adhered to the daughter cell wall. In *N. bacillaris*, the cleaved mother cell wall gradually degenerated and was not observed in the next cell cycle. In contrast, *M. geminata* daughter cells entered the growth phase of the next cell cycle bearing the mother and grandmother cell walls, causing the uncovered portion of the plane of division to bulge outward. Such a delay in the degeneration and shedding of the mother cell wall probably led to the development of binary fission and budding.

Keywords Autosporulation · Binary fission · Budding · Cell wall · *Marvania* · *Nannochloris*

M. Yamamoto (✉)
Institute of Natural Sciences, Senshu University,
2-1-1, Tama, Kawasaki, Kanagawa 214-8580, Japan
e-mail: yamamoto@isc.senshu-u.ac.jp

T. Nishikawa · H. Kajitani · S. Kawano
Department of Integrated Biosciences,
Graduate School of Frontier Sciences,
University of Tokyo, Kashiwa, Chiba, Japan

Introduction

In plant cells that are enveloped by rigid cell walls, daughter cells are generated within the space enclosed by the mother cell wall. The existence of cell walls probably led to the present diversity of plant cell division methods. For example, unicellular green algae of the Trebouxiophyceae or Chlorophyceae generally multiply via autosporulation, whereas cell division in other green algae such as *Spirogyra* (Charophyceae) involves the formation of an actin ring followed by the inward growth of a furrow at the cell surface that ultimately leads to the development of a small cell plate at the center of the dividing plane (McIntosh et al. 1995). In comparison, terrestrial plants divide via cell plate formation. The various modes of plant cell division are useful for taxonomy and phylogeny, but they also provide clues concerning the evolution of multicellular higher plants from unicellular green algae.

The class Trebouxiophyceae, which contains the representative genera *Chlorella*, *Parachlorella*, and *Trebouxia*, are non-flagellated vegetative cells that propagate mainly by autosporulation. *Nannochloris bacillaris*, a long, ellipsoidal, binary-fission-type species first described by Naumann (1921), is also a member of the Trebouxiophyceae (Yamamoto et al. 2001, 2003). In classifying *N. bacillaris*,

Naumann (1921) also included in the genus *Nannochloris* a small species that divides by binary fission, *Nannochloris coccoides*. *N. bacillaris* NRJ propagates by binary fission, whereas *N. coccoides* CCAP251/1B (Trebouxiophyceae; Yamamoto et al. 2001, 2003) propagates by budding (Tschermak-Woess 1999). Similarly, *Marvania geminata*, a budding type species identified by Hindák (1976), is also included in the Trebouxiophyceae (Henley et al. 2004). Tschermak-Woess (1999) insisted that *N. coccoides* CCAP251/1B is really *M. geminata* and not a *Nannochloris* species. The Culture Collection of Algae at the University of Göttingen, Germany (SAG), maintains stocks of *M. geminata* SAG 12.88 and *M. geminata* SAG 13.96, although the latter is referred to as *N. coccoides* CCAP251/1B in the Culture Collection of Algae and Protozoa, UK (CCAP).

Recently, species classified into the genus *Nannochloris*, i.e., *N. bacillaris*, *N. coccoides* CCAP251/1B, *N. atomus* CCAP251/7 and SAG 14.87, *N. maculatus*, *N. eucaryotum*, *N. oculata*, and some unidentified *Nannochloris* species, were confirmed as Trebouxiophyceae (Yamamoto et al. 2001, 2003; Henley et al. 2004). Phylogenetic analyses based on the actin and 18S rRNA sequences in several *Chlorella*, *Parachlorella*, and *Trebouxia* species indicated that five autospore-forming strains, that is, *N. atomus* CCAP251/7 and SAG 14.87, *N. maculatus*, *N. eucaryotum*, and *N.* sp. SAG 251-2, are polyphyletic, whereas *N. bacillaris* and *N. coccoides* CCAP251/1B are monophyletic and positioned distally (Yamamoto et al. 2003). These results indicate that autosporulation is the ancestral mode of cell division in the Trebouxiophyceae. Non-autosporulative mechanisms such as binary fission and budding would therefore have evolved secondarily. If *N. coccoides* CCAP251/1B is actually *M. geminata*, as suggested by Tschermak-Woess (1999), the phylogenetic position of *N. coccoides* CCAP251/1B and *M. geminata* should be the same, and both species should be closely related to *N. bacillaris*. A phylogenetic analysis by Henley et al. (2004) based on existing and new 18S rRNA sequences from multiple *Nannochloris* species, their related isolates, and numerous other members of the Trebouxiophyceae, grouped *N. coccoides* CCAP251/1B with *M. geminata*. The inclusion of numerous related taxa revealed genus-level divergence of *N. bacillaris* and *N. coccoides* CCAP251/1B, but both were assigned to the "freshwater group." Henley et al. (2004) proposed including *N. atomus* CCAP251/7, *N. eucaryotum* Mainz1, *N. oculata* UTEX 1998, *N. maculatus* CCAP251/3, and some unidentified *Nannochloris* species in the new genus *Picochlorum*. According to Henley's diagnosis, *Picochlorum* species grow in moist soil or water (either saline or fresh) and *Picochlorum* is a sister group of the freshwater group in the 18SrRNA tree (Henley et al. 2004). However, *N. bacillaris*, *N. coccoides* CCAP251/1B, and *M. geminata* were assigned to the freshwater group. On the basis of these results, Henley et al. (2004) renamed *N. coccoides* CCAP251/1B as *Marvania coccoides*. We reconfirmed the phylogeny of *M. coccoides* CCAP251/1B and *M. geminata* SAG 12.88 by constructing a phylogenetic tree based on their actin gene sequences.

By focusing on the relative timing of mother cell wall cleavage and daughter cell wall formation in *N. bacillaris* and *M. geminata* SAG 12.88, we sought to understand the relationship between these two species and how their distinct methods of cell division emerged from the ancestral mode of autosporulation. In autosporulation, daughter cells, which have their own walls enveloping their protoplasts, are formed inside the wall of the mother cell. In *Chlorella vulgaris*, *Chlorella sorokiniana*, and *Chlorella lobophora*, which belong to the Trebouxiophyceae, daughter cell wall formation begins at the outer surface of the cell membrane prior to protoplast division. During the division of the protoplast, the daughter cell wall invaginates with the plasma membrane at a cleavage furrow (early synthesis type of daughter cell wall; see Yamamoto et al. 2004). In contrast, in *Parachlorella kessleri*, which also belongs to the Trebouxiophyceae, synthesis of the daughter cell wall begins at the outer surface of the plasma membrane in the daughter protoplast at the autospore-maturing phase after three successive protoplast divisions (late synthesis type of daughter cell wall; see Yamamoto et al. 2005). In both cases, as the synthesis of the daughter cell wall nears completion, the mother cell wall bursts and the daughter cell emerges with its own wall.

To observe changes in cell wall structure during the cell cycle in *N. bacillaris* and *M. geminata*, we used Fluostain I, a cell wall-specific fluorescent dye. We also used transmission electron microscopy with rapid freezing and freeze substitution to observe the structure of the cell walls in detail. We found that the timing of mother cell wall cleavage and exfoliation greatly influences the mode of cell division.

Materials and methods

Algal culture

Nannochloris bacillaris NRJ was collected from Lake Nakatuna in Nagano Prefecture by Dr. N. Takamura of the National Institute for Environmental Studies at Tsukuba, Japan (Ogawa et al. 1995; Arai et al. 1998; Yamamoto et al. 2001) and was given to us by Prof. K. Ueda of Nara Women's University (NRJ). *M. coccoides* CCAP251/1B was purchased from CCAP in 1998. *M. geminata* SAG 12.88 was purchased from SAG in 2002. The species were cultured in modified Ichimura's C medium (Chida and Ueda 1991) and grown under continuous light (15 μmol photons m^{-2} s^{-1}) at 23°C.

Light microscopy

Dividing cells were observed under differential interference contrast microscopy (BX52, Olympus, Tokyo, Japan). Cells were harvested by centrifugation at 3,300 × *g* for 1 min and double-stained with 0.001% Fluostain I (Dojindo, Kumamoto, Japan) and 0.003% SYBR Green I (Molecular Probes, Eugene, OR, USA) in PBS buffer (0.13 M NaCl, 7 mM Na_2HPO_4, 3 mM NaH_2PO_4, and pH 7.2). The stained samples were examined first using differential interference and phase-contrast optics for light-field images, and then under ultraviolet excitation for Fluostain I, blue excitation for SYBR Green I, and green excitation for chlorophyll autofluorescence, using a BX52 microscope (Olympus) equipped with a c4742 CCD camera (Hamamatsu Photonics Co., Shizuoka, Japan) and an AQUACOSMOS system (Hamamatsu Photonics Co.). An Olympus Apo 100 × objective was used in combination with a U-25ND25 filter and U-MNUA2 band-pass cube.

DNA extraction and actin sequencing

Total DNA was extracted from *M. geminata* SAG 12.88 and *C. lobophora* using the Easy-DNA Kit (Invitrogen Life Technologies, Carlsbad, CA, USA) according to the manufacturer's instructions. A degenerate PCR method was used to isolate actin gene fragments from *M. geminata* SAG 12.88 and *C. lobophora* (Yamamoto et al. 2003). Each PCR product was ligated into the pGEM-T-Easy vector (Promega, Madison, WI, USA). The nucleotide sequences were determined according to Yamazaki et al. (2005), and have been submitted to DDBJ/EMBL/GenBank under accession numbers AB292587 and AB292588 for *M. geminata* SAG 12.88 and *C. lobophora*, respectively.

Phylogenetic analysis of the actin gene sequences

The nucleotide sequences of the actin genes from *M. geminata* SAG 12.88 and *C. lobophora* were used for phylogenetic analysis, along with the published sequences from *N. bacillaris* (Arai et al. 1998), *M. coccoides* CCAP251/1B, *N. eucaryotum* KSW 0203 (a single colony was isolated from UTEX 2502, Yamamoto et al. 2003), *N. atomus* SAG 14.87, *N.* sp. SAG 251-2., *Picochlorum atomus* CCAP251/7, *P. kessleri* IAM C-531 (Yamamoto et al. 2001), *C. vulgaris* IAM C-536, *C. sorokiniana* IAM C-212, and *Trebouxia erici* IAM C-593 (Yamamoto et al. 2003). Between 674 and 762 bp of the coding regions from the actin genes in each organism were unambiguously aligned. The first and second positions were used exclusively because of mutational saturation at the third position (Bhattacharya et al. 1991). To test alternative models of evolution for these data, we used PAUP 4.0 beta 10 (Swofford 2002) and Modeltest 3.07 (Posada and Crandall 1998). The tree was constructed using the best fit model (JC + G and $\gamma = 0.1805$) selected using hierarchical likelihood ratio testing (hLRT) and the maximum likelihood (ML) algorithm. The robustness of the resulting lineages was tested using bootstrap analysis. The number of bootstrap replicates was 1,000 (minimum evolution) and 1,000 (maximum parsimony). Using the alignment data, a ML analysis was also carried out to estimate quartet puzzling support values with 1,000 puzzling steps. Because Trebouxiophyceae is a sister group of Chlorophyceae within the Chlorophyta (Friedl 1995), the chlorophycean algae *Volvox* and *Chlamydomonas* were used as outgroups.

Transmission electron microscopy

Cultured cells of *N. bacillaris* and *M. geminata* SAG12.88 were fixed using rapid freeze fixation and freeze substitution and observed using transmission electron microscopy. Rapid freezing was performed according to the method of Baba and Osumi (1987), with minor modifications. Cells were harvested by centrifugation at 3,300 × *g* for 1 min and then rapidly frozen in liquid propane that had been cooled to −185°C with liquid nitrogen using a Leica EM CPC cryoworkstation (Leica Mikrosystems, Vienna, Austria). The frozen cells were transferred to 2.5% glutaraldehyde in dry acetone at −80°C and incubated at −80°C for 108 h. Subsequently, the samples were warmed gradually from −80 to 0°C over 5 h, held at 0°C for 1 h, warmed from 0 to 23°C over 1 h, and incubated at 23°C for 1 h (Leica EM AFS, Leica Mikrosystems). The samples were washed three times with dry acetone at room temperature and transferred to 2% OsO_4 in dry acetone at 40°C for 4 h. The samples were then washed three times with dry acetone at room temperature and infiltrated with increasing concentrations of Spurr's resin (Spurr 1969) in dry acetone, and finally with 100% Spurr's resin. Ultrathin sections (0.06–0.07 μm) were cut using a diamond knife on an ultramicrotome (Leica Ultracut UCT, Leica Mikrosystems) and mounted on Formvar-coated copper grids. The sections were stained with 3% uranyl acetate for 2 h at room temperature and with lead citrate for 10 min at room temperature, washed in distilled water, and examined using an electron microscope (H-7600, Hitachi Co., Tokyo, Japan) at 100 kV.

Results

Cell morphology compared to original descriptions of *N. bacillaris*, *M. coccoides*, and *M. geminata*

As described by Naumann (1921), *N. bacillaris* is ellipsoidal (1.5 μm in width and 3–3.5 μm in length), grows to a

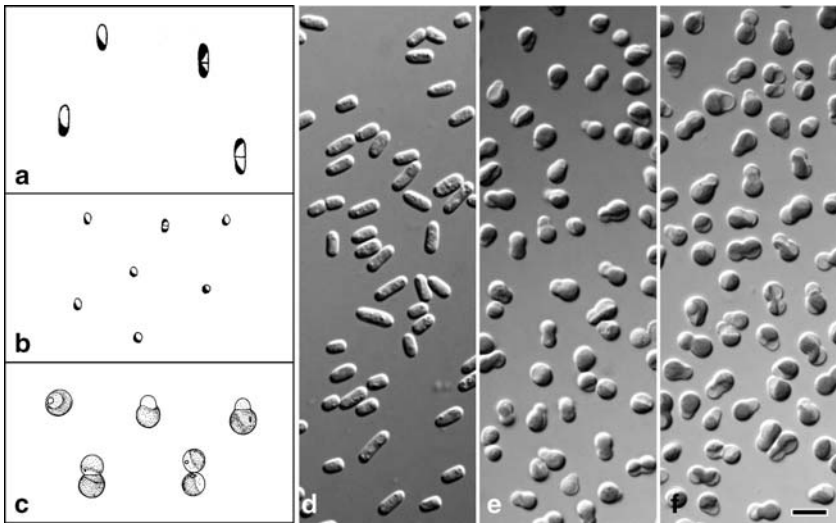

Fig. 1 Modes of cell division in *Nannochloris bacillaris*, *Marvania coccoides* CCAP251/1B, and *Marvania geminata* SAG 12.88. **a** *Nannochloris bacillaris* and **b** *Nannochloris coccoides* as shown in Naumann's (1921) original descriptions; they propagate by binary fission. **c** *Marvania geminata* as shown in Hindák's (1976) original description; it propagates by budding. **d** Differential interference image of *N. bacillaris* propagating by binary fission. **e** Differential interference image of *M. coccoides* CCAP251/1B propagating by budding. **f** Differential interference image of *M. geminata* SAG 12.88 propagating by budding. Scale bar 5 μm

length of 5–6 μm, and divides by binary fission (Fig. 1a, d). In comparison, *M. coccoides* CCAP251/1B is spherical (3–3.2 μm in diameter) and divides by budding (Fig. 1e). Thus, the morphology and mode of cell division observed do not coincide with Naumann's (1921) description (Fig. 1b). *M. geminata* SAG 12.88 is spherical (3.5–3.8 μm in diameter) and divides by budding (Fig. 1f), which coincides with Hindák's (1976) description (Fig. 1c). Our observations indicate that the morphology and mode of cell division in *M. coccoides* CCAP251/1B match those of *M. geminata* SAG 12.88.

Phylogenetic analysis using actin gene sequences

We amplified conserved regions of the actin gene in *M. geminata* SAG 12.88 by degenerate PCR. The sequence of the 674-bp amplified fragment was identical with the sequence reported for *M. coccoides* CCAP251/1B. The first and second codon positions of the sequences from *M. geminata* and *M. coccoides* were used for ML phylogenetic analysis, together with actin gene sequence data from several *Nannochloris*, *Chlorella*, and *Trebouxia* species (Fig. 2). *M. geminata* SAG 12.88 and *M. coccoides* CCAP251/1B were positioned at the same site, indicating that they belong to the same genus.

SYBR Green I/Fluostain I double-staining in cells undergoing binary fission and budding

To compare the process of daughter cell wall synthesis in *N. bacillaris* and *M. geminata* SAG 12.88, we observed SYBR Green I/Fluostain I double-stained cells at each stage of the cell cycle. Progress through the cell cycle was judged by SYBR Green I staining of the cell nuclei and the chlorophyll autofluorescence, whereas the synthesis of daughter cell walls was detected by Fluostain I fluorescence.

In *N. bacillaris*, growth-phase cells were identified by SYBR Green I staining of the single nucleus found at the right side of the image (Figs. 3c, 4c) and autofluorescence of a chloroplast that occupied the lower side of the image (Figs. 3d, 4d). In the early growth phase, strong Fluostain I fluorescence was observed only at the rim on the right side of the image (Fig. 3e). Later in the growth phase, very weak Fluostain I fluorescence was detected throughout the entire cell (Fig. 4e). During protoplast division, the nucleus was situated near the middle of the cell (Fig. 5c). The chloroplast then divided in half (Fig. 5d) and nuclear division followed (Fig. 6c). Strong Fluostain I fluorescence was observed at the plane of division (Fig. 6e). Ultimately, the two daughter cells separated along the plane of division (Figs. 7, 8). No fluorescence was observed in the mother cell wall (Figs. 3e–8e).

In *M. geminata* SAG 12.88, cells at the early growth phase were spherical (diameter 3.5–3.8 μm; Fig. 9), with SYBR Green I staining in one nucleus (Fig. 9c) and autofluorescence in one semi-circular chloroplast that occupied half of the cell (Fig. 9d). Fluostain I fluorescence was observed at the edges of each cell. In addition, strong fluorescence was observed at the upper and lower right-hand side of the image (Fig. 9e). Each cell expanded by budding (Figs. 10, 11, 12) from the site of strong Fluostain I fluorescence to the right side of the image (Figs. 10e–12e). The

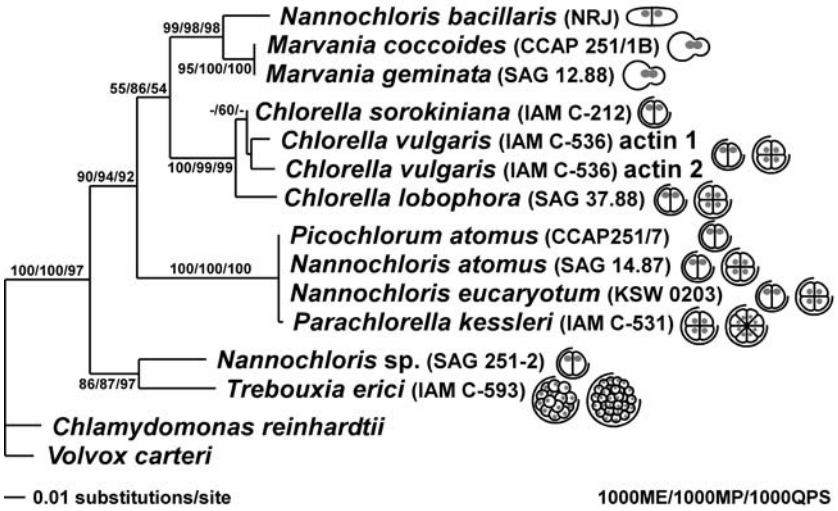

Fig. 2 Phylogenetic analysis of the actin-coding regions of *Nannochloris* and *Marvania*. A phylogenetic tree was constructed using the maximum likelihood (*ML*) algorithm in PAUP 4.0 b10. Only the first and second positions of the actin codons were used. Twelve species of Trebouxiophyceae were used as the ingroup; *Chlamydomonas reinhardtii* and *Volvox carteri* were used as outgroups. The *numbers* are bootstrap values (≥50%) based on 1,000 replicates of minimum evolution (*ME*) and maximum parsimony (*MP*), and quartet puzzling support values (≥50%) based on ML analyses with 1,000 puzzling steps, respectively. The modes of cell division are illustrated on the phylogenetic tree

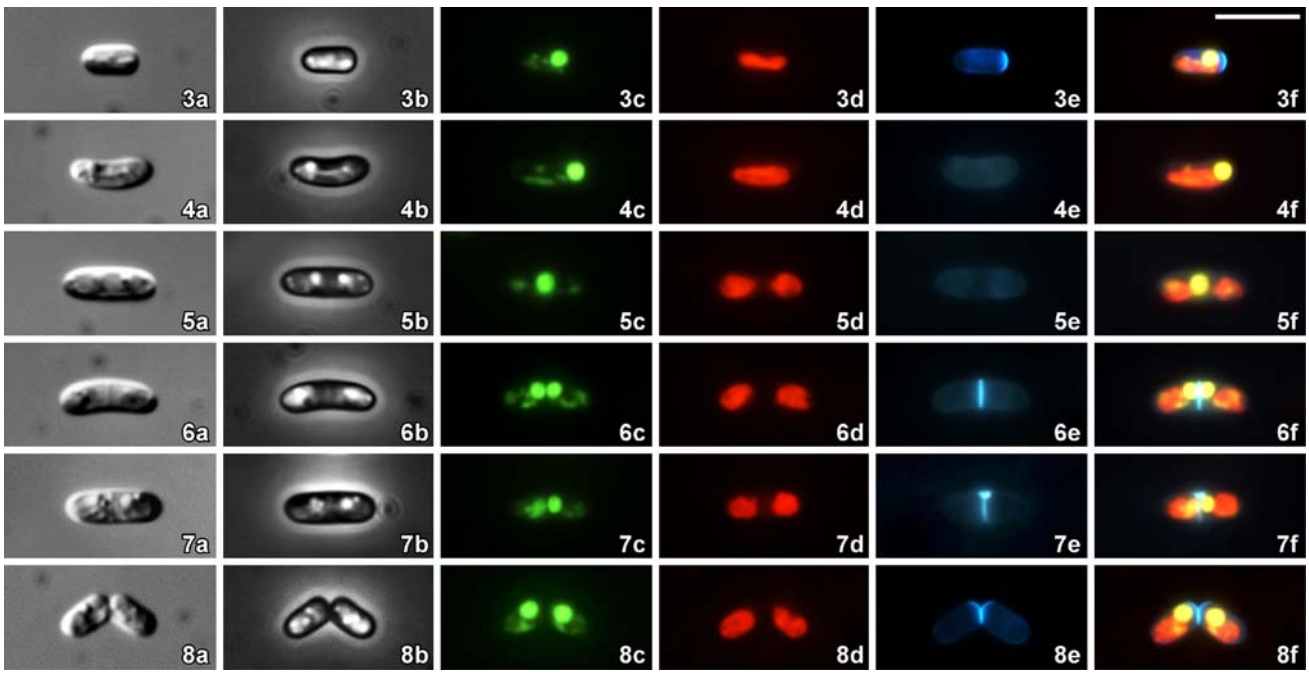

Fig. 3-8 Cell wall development during the cell cycle in *Nannochloris bacillaris*. Living cells were observed after double-staining with SYBR Green I and Fluostain I. Photographs, from top to bottom, show the progression of the cell cycle. Fig. **3**, Early growth phase; Fig. **4**, Late growth phase; Fig. **5**, Chloroplast division; Fig. **6**, Nuclear division; Fig. **7**, Protoplast division; Fig. **8**, Daughter cell separation. Figs. **3a**–**8a**, Differential interference images; Figs. **3b**–**8b**, Phase contrast images; Figs. **3c**–**8c**, SYBR Green I fluorescence; Figs. **3d**–**8d**, Chlorophyll autofluorescence; Figs. **3e**–**8e**, Fluostain I fluorescence; Figs. **3f**–**8f**, Merged SYBR Green I fluorescence/autofluorescence/Fluostain I fluorescence images. In the false-color images (**c**–**f**), DNA is stained *green* with SYBR Green I, cell walls are stained *whitish-blue* with Fluostain I, and chlorophyll autofluorescence appears *red*. *Scale bar* 5 μm

cells grew to 5.8–6.0 μm in length, doubling in volume and assuming a dumbbell shape (Fig. 12). During cell division, the chloroplast divided in half (Fig. 13d), followed by the halving of the nucleus (Fig. 14c). During division of the protoplast, a belt of Fluostain I fluorescence was observed at the budding site (i.e., at the plane of division), which was

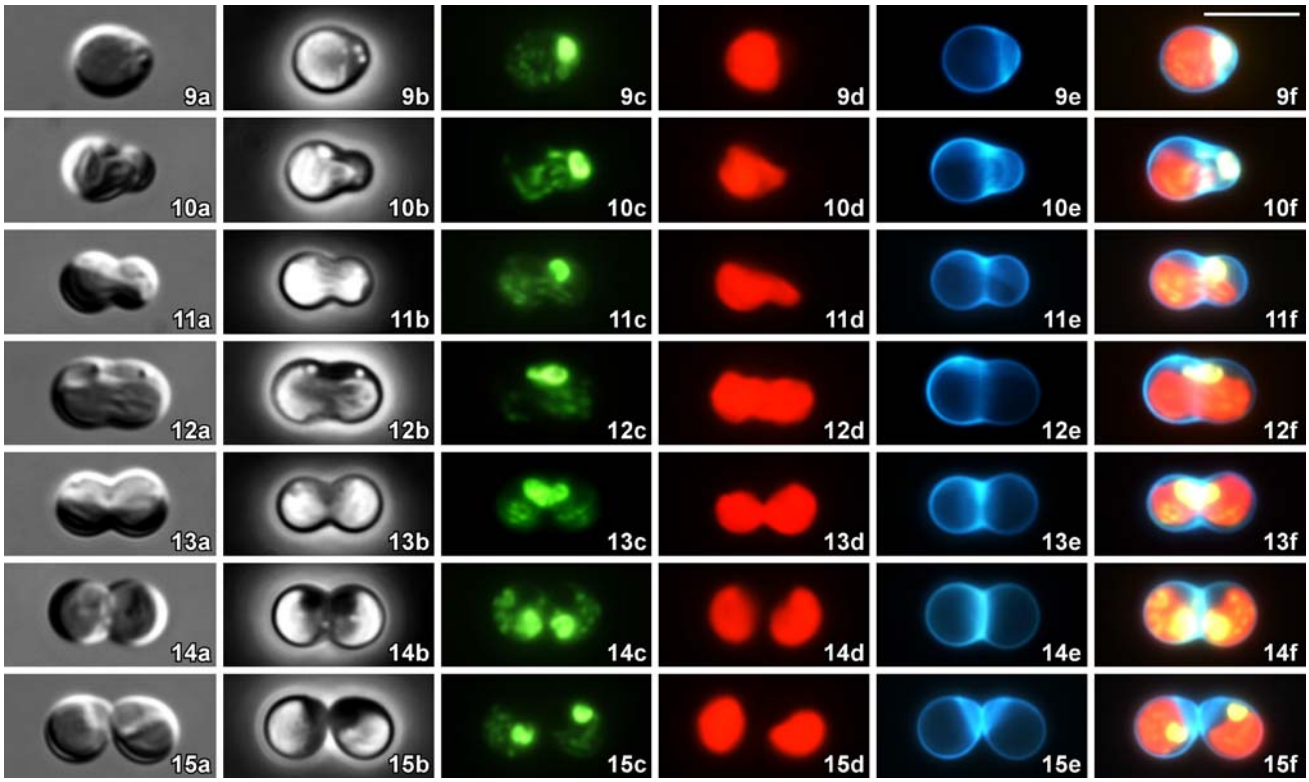

Fig. 9-15 Cell wall development during cell division in *Marvania geminata* SAG 12.88. Living cells were observed after double-staining with SYBR Green I and Fluostain I. Photographs, from top to bottom, show the progression of the cell cycle. Fig. **9**, Early growth phase; Fig. **10**, Late growth phase I (the bud is growing); Fig. **11**, Late growth phase II (the bud becomes larger); Fig. **12**, Chloroplast division; Fig. **13**, Nuclear division; Fig. **14**, Protoplast division; Fig. **15**, Daughter cell separation. Figs. **9a**–**15a**, Differential interference images; Figs. **9b**–**15b**, Phase contrast images; Figs. **9c**–**15c**, SYBR Green I fluorescence; Figs. **9d**–**15d**, Chlorophyll autofluorescence; Figs. **9e**–**15e**, Fluostain I fluorescence; Figs. **9f**–**15f**, Merged SYBR Green I fluorescence/autofluorescence/Fluostain I fluorescence images. In the false-color images (**c**–**f**), DNA is stained *green* with SYBR Green I, cell walls are stained *whitish-blue* with Fluostain I, and chlorophyll autofluorescence appears *red*. *Scale bar* 5 μm

at the same position as the strong fluorescence observed during the growth phase (Figs. 13e, 14e). Thereafter, the two daughter cells separated (Fig. 15).

Fluorescence of the mother cell wall was not observed in either *N. bacillaris* or *M. geminata* SAG 12.88. In contrast, a strong Fluostain I signal at the plane of division was a characteristic feature of both the binary fission and budding type cells.

Daughter cell wall regeneration and mother cell wall exfoliation in *N. bacillaris*

In autosporulation, the cell sheds its outermost layer (i.e., the mother cell wall) during each round of cell division. We did not observe shedding of the mother cell wall in either binary fission or budding. Further, the strong Fluostain I signal observed at the plane of division was common to both species, suggesting that active daughter cell wall synthesis occurs there. Based on these results, we used electron microscopy in combination with rapid freeze fixation and freeze substitution to explore daughter cell wall regeneration and mother cell wall exfoliation.

During the early growth phase of *N. bacillaris*, each cell was ellipsoidal in shape with a large ellipsoidal chloroplast and a nucleus positioned at one end of the cell (Fig. 16a). Later in the growth phase, the cell elongated with the chloroplast (Fig. 16b), and a cell wall was observed (cw1, the outer electron-dense layer; Fig. 16e, f). During protoplast division (Fig. 16c), invagination of the plasma membrane was observed at the plane of division (Fig. 16g), and synthesis of the daughter cell wall on the plasma membrane had not yet begun (Fig. 16d, i). This suggests that the daughter cell wall is not synthesized by the time the protoplast completes division (Fig. 16j).

Instead, shortly after protoplast division, a thin daughter cell wall (i.e., cw2) was synthesized between the invaginated plasma membranes at the plane of division (Fig. 17a, e, f) and gradually increased in thickness (Fig. 17b, g, h). A triangular space was observed between cw1 and cw2 (Fig. 17f, h, arrows); the space was smaller than that observed

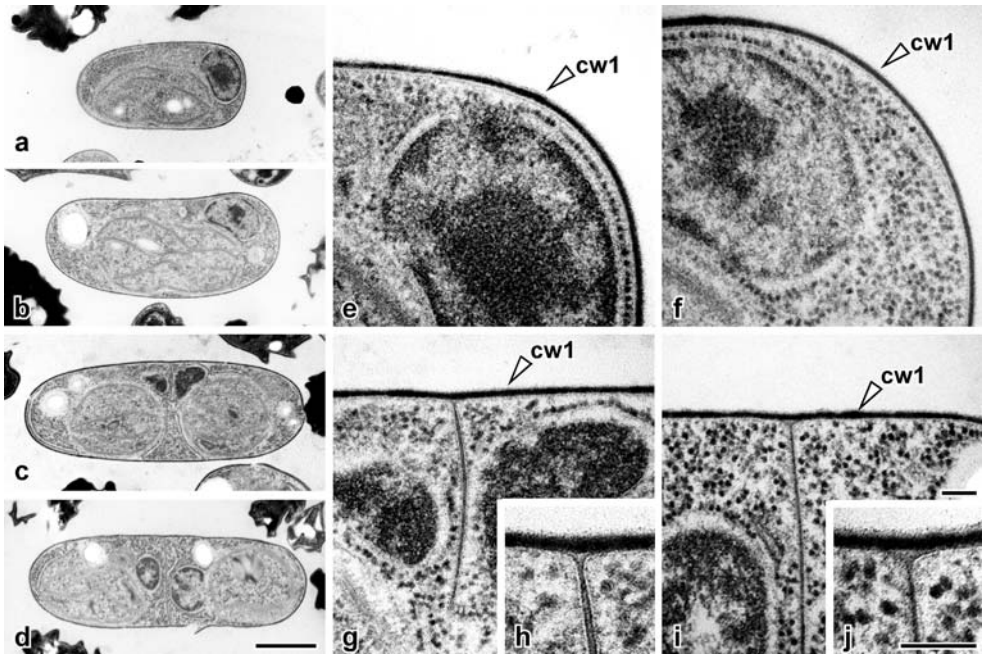

Fig. 16 Transmission electron micrographs of *Nannochloris bacillaris* in the growth phase (**a**, **b**, **e**, and **f**) and during protoplast division (**c**, **d**, and **g**–**j**). **a** A whole cell in the early growth phase, **b** a whole cell in the late growth phase, **c** a whole cell showing invagination of the plasma membrane, **d** a whole cell after invagination of the plasma membrane, **e** highly magnified view of the cell wall in **a**, **f** highly magnified view of the cell wall in **b**, **g** highly magnified view of the plane of division in **c**, **h** the site of invagination of the plasma membrane at the cell surface in **g**, **i** highly magnified view of the plane of division in **d**, **j** the site of invagination of the plasma membrane at the cell surface in **i**. *Scale bar* 1 μm (**d**) and 100 nm (**i** and **j**)

during autosporulation, so it could not be observed under light microscopy. Because the daughter cell wall (cw2) was newly synthesized, cw1 is hereafter called the mother cell wall. The mother cell wall was cleaved at the triangular space (Fig. 17c) on the upper side of the image (Fig. 17i), whereas the lower side remained intact (Fig. 17j).

After cleavage of the mother cell wall, the daughter cell divided into two from the upper side of the plane of division (Fig. 17d). The plane of division then separated, exposing cw2 to the outside (Fig. 17k). Strong Fluostain I signals were detected at these positions (Fig. 3e). However, cw1 did not separate from the daughter cell; instead, it remained adhered to cw2. A scar from the cleavage of cw1 remained on the surface of the daughter cell just after cell division (Fig. 17k, arrow). The cleaved mother cell wall degenerated gradually and was not observed in the next growth phase (Fig. 16e, f).

Daughter cell wall regeneration and multiple mother cell wall layers in *M. geminata*

Early in the growth phase, *M. geminata* was spherical (Fig. 18a) with a multilayered cell wall. The cw1 enclosed the entire cell and was overlaid by the grandmother cell wall (cw0); however, cw0 did not completely enclose the entire cell (Fig. 18e). Breaks were detected that seemed to coincide with strong Fluostain I fluorescence (see Fig. 9e). In the budding cell, the bud was not covered by cw0 (Fig. 18b). Instead, the cell grew from a site that was free from remnants of the cleaved cw0 (Fig. 18f). Following protoplast division, cw2 gradually increased in thickness between the invaginated plasma membrane (Fig. 18c). The cw1 is hereafter called the mother cell wall (Fig. 18g). Although the triangular space between cw1 and cw2 was not obvious, cw1 was cleaved at that position and the daughter cells separated at the plane of division (Fig. 18d). Consequently, the daughter cell on the left side of the image was covered by cw2, cw1, and cw0; the daughter cell on the right side was covered by cw2 and cw1 (Fig. 18h). The two daughter cells were consistently asymmetrical in terms of their cell wall formation. The mother cell wall was not exfoliated as in autosporulation, and it did not degenerate as in *N. bacillaris*. The daughter cells entered the next growth phase still carrying the mother cell wall or grandmother cell wall, causing the uncovered portion of the cell to bud outward.

Discussion

We reconfirmed that in *M. coccoides* CCAP251/1B (Fig. 1e), cell division does not occur as described by Naumann (1921; Fig. 1b). In addition, the results of our phylogenetic analysis using actin sequence data from several species,

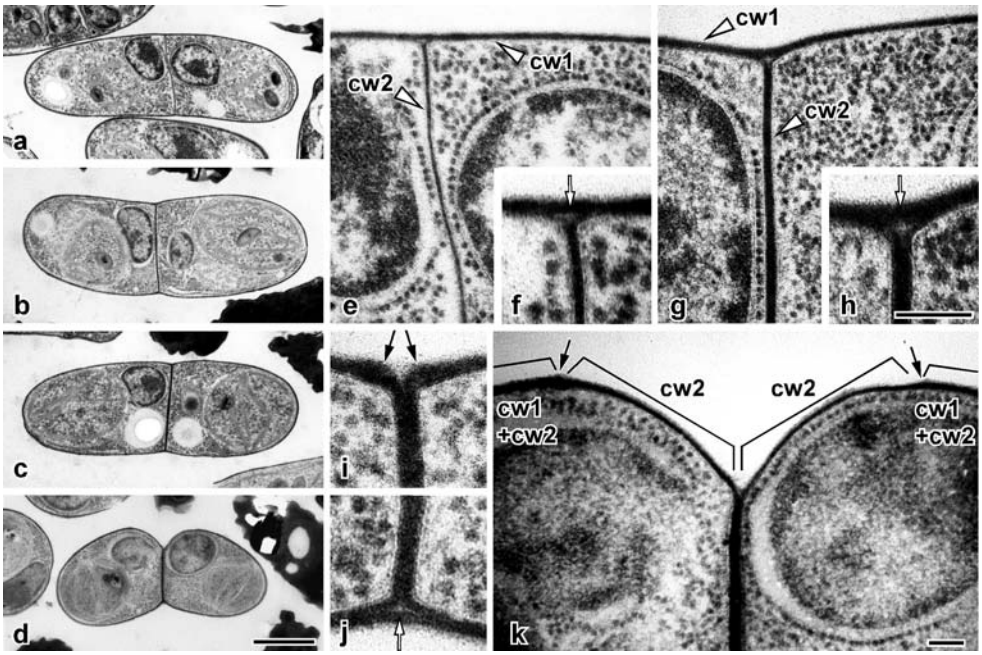

Fig. 17 Transmission electron micrographs of *Nannochloris bacillaris* during formation of the daughter cell wall (**a**, **b**, and **e**–**h**) and during separation of the daughter cells (**c**, **d**, and **i**–**k**). **a** A whole cell during early daughter cell wall formation, **b** a whole cell during late daughter cell wall formation, **c** a whole cell showing cleavage of the mother cell wall at the plane of division, **d** a whole cell showing the separation of the daughter cells, **e** highly magnified view of the cell wall at the plane of division in **a**, **f** the plane of division at the cell surface in **e**, **g** highly magnified view of the cell wall at the plane of division in **b**, **h** the plane of division at the cell surface in **g**, **i** highly magnified image of **c** at the upper side of the plane of division, **j** highly magnified image of **c** at the lower side of the plane of division, **k** highly magnified view of **d** at the plane of daughter cell separation. *Scale bar* 1 μm (**d**) and 100 nm (**h** and **k**). *White arrows*, triangular space; *black arrows*, cleavage site of cw1

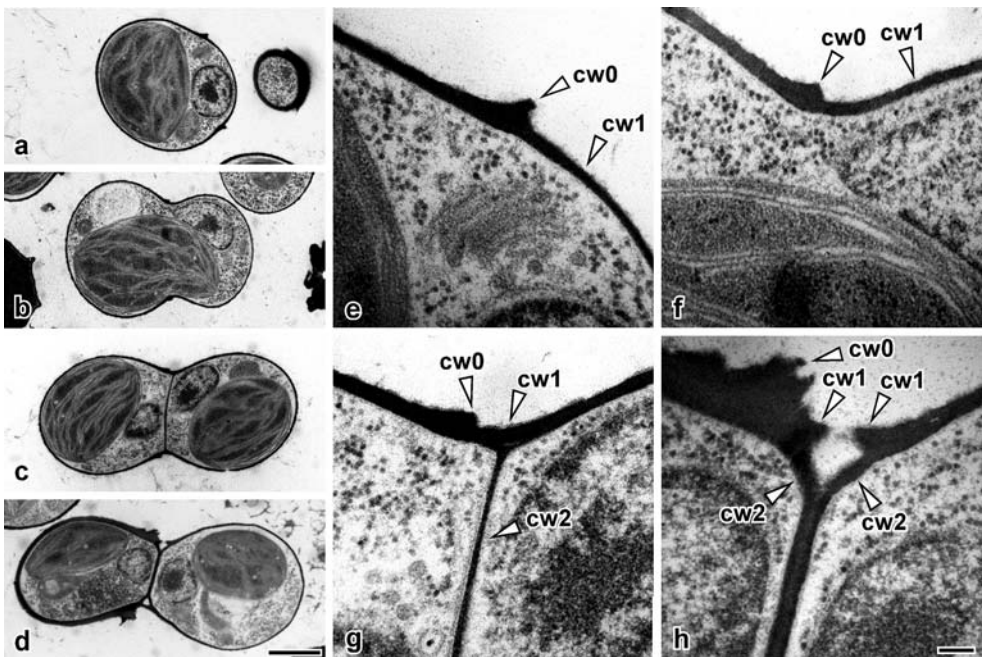

Fig. 18 Transmission electron micrographs of *Marvania geminata* SAG 12.88 during the growth phase (**a**, **b**, **e**, and **f**) and during cell division (**c**, **d**, **g** and **h**). **a** A whole cell in the early growth phase, **b** a whole cell in the bud-forming phase, **c** a whole cell during formation of the daughter cell wall after protoplast division, **d** a whole cell during separation of the daughter cells after cleavage of the mother cell wall, **e** and **f** highly magnified views of the cell walls in **a** and **b** at the budding site, **g** and **h** highly magnified views of the cell walls in **c** and **d** at the plane of division. *Scale bar* 1 μm (**d**) and 100 nm (**h**)

including *M. geminata* SAG 12.88, indicate that *M. coccoides* CCAP251/1B and *M. geminata* SAG 12.88 are located in the same position. Tschermak-Woess (1999) insisted that *N. coccoides* CCAP251/1B (i.e., *M. coccoides*) is not a *Nannochloris* species, but that it is actually *M. geminata* (Hindák 1976; Fig. 1c), which reproduces by budding. The 18S rRNA sequence data from *M. geminata* SAG 12.88 was submitted to DDBJ/EMBL/GenBank by Bhattacharya et al. (1999; accession number AF124336). Henley et al. (2004) used 18S rRNA sequence data to construct a detailed phylogenetic tree that included *M. geminata* SAG 12.88 and a new isolate, *M.* sp. JL11-11. Our results indicate that these species are all close relatives. There are differences in cell size, cultured cell buoyancy, and extracellular polysaccharide distribution between *M. coccoides* CCAP251/1B and *M. geminata* SAG12.88. It is thus appropriate that Henley et al. (2004) renamed *N. coccoides* CCAP251/1B as *M. coccoides.* Among the strains presently available, *N. bacillaris* is the only "true" *Nannochloris* species that matches Naumann's (1921) original description (i.e., is ellipsoidal in shape and propagates by binary fission).

Henley et al. (2004) proposed including *N. atomus* CCAP251/7 in the new genus *Picochlorum*, with some other *Nannochloris* species. However, *N. atomus* SAG 14.87 and *N. eucaryotum* UTEX 2502 were excluded from *Picochlorum* because of markedly different 18SrRNA sequences. However, in this study, the actin tree suggests a close relationship among these three species, *P. atomus* CCAP251/7, *N. atomus* SAG 14.87, and *N. eucaryotum* UTEX 2502 (Fig. 2). The incongruity between the actin and 18SrRNA trees was discussed in Yamamoto et al. (2003).

The stilbene-derived fluorescent dye Fluostain I has been used extensively to study plant morphogenesis (Belliveau et al. 1990). It is possible to visualize the cell walls of live Trebouxiophyceae by fluorescent microscopy using Fluostain I. In the case of autosporulation, one can observe both the fluorescence of the daughter cell wall, as well as the sloughing of the mother cell wall by staining cells in the hatching phase (Yamamoto et al. 2004). Shedding of the mother cell wall is relatively difficult to observe by transmitted light, but it is easily observed by Fluostain I staining. However, we observed no sloughing of the mother cell wall in *N. bacillaris* and *M. geminata*. Shedding of the mother cell wall is not a common feature of binary fission and budding. The primary difference between binary fission/budding and autosporulation is whether the mother cell wall is shed; however, there are other differences between binary fission and budding. For example, in *M. geminata*, a budding type alga, we were unable to differentiate the mother cell wall from the daughter cell wall; a fluorescent signal was observed across the entire cell. In contrast, in *N. bacillaris*, the newly formed cell wall at the plane of division displayed a stronger signal than any other area in the cell. Moreover, we observed spots of strong fluorescence at the growth phase during budding that were never observed during binary fission.

Sluiman and Reymond (1987) observed mitosis and cytokinesis in chemically fixed *M. geminata* using electron microscopy. They demonstrated that after the formation of the new wall layers at the septum, the mother cell wall that encloses the two daughter cells breaks at the position of the septum. They reported that the pattern of cell division in *M. geminata* appeared to be more similar to that of the Chlorococcales than suggested by initial light microscopic observations (Hindák 1976). They also noted that a better description of cell division in *M. geminata* may be "semi-exogenous formation of autospore diads" (Sluiman and Reymond 1987).

We observed *N. bacillaris* and *M. geminata* SAG 12.88 using electron microscopy in combination with rapid freeze fixation and freeze substitution. Formation of the daughter cell wall and cleavage of the mother cell wall occurred at the plane of division, and the two daughter cells separated. This sequence of events corresponds to the term "semi-exogenous formation of autospore diads." Because the daughter cell remains covered by the remnants of the cleaved mother cell wall, the growth of the daughter cell proceeds by expansion from a site not covered by mother cell wall. This results in bulging or budding of the growing cell. It has been suggested that the essential processes of cell division (i.e., protoplast division, daughter cell wall synthesis, and cleavage of the mother cell wall) are the same as in autosporulation. Indeed, some members of the genus *Marvania*, which includes the subaerial tropical green alga *M. aerophytica* (Neustupa and Šejnohová 2003), reproduce via a type of budding that has been described as highly modified autosporulation.

Our phylogenetic analysis and transmission electron microscopy observations indicate that non-autosporic cell division arose from the autosporic mode due to the loss of shedding of the mother cell wall. This process likely involved a series of evolutionary events. For example, a mode of cell division that did not involve hatching of the daughter cell may have been followed by a mode in which the mother cell wall gradually degenerated during the subsequent growth phase (binary fission), until finally, a mode emerged in which the cleaved mother cell wall remained covering the daughter cell during the next growth phase (budding; Fig.19). An essential difference between autosporulation and non-autosporulative binary fission and budding is whether the mother cell wall is shed. In addition, a difference in the onset of mother cell wall degeneration distinguishes binary fission from budding. During binary fission in *N. bacillaris*, the daughter cell wall does not form during the invagination of the plasma membrane at the

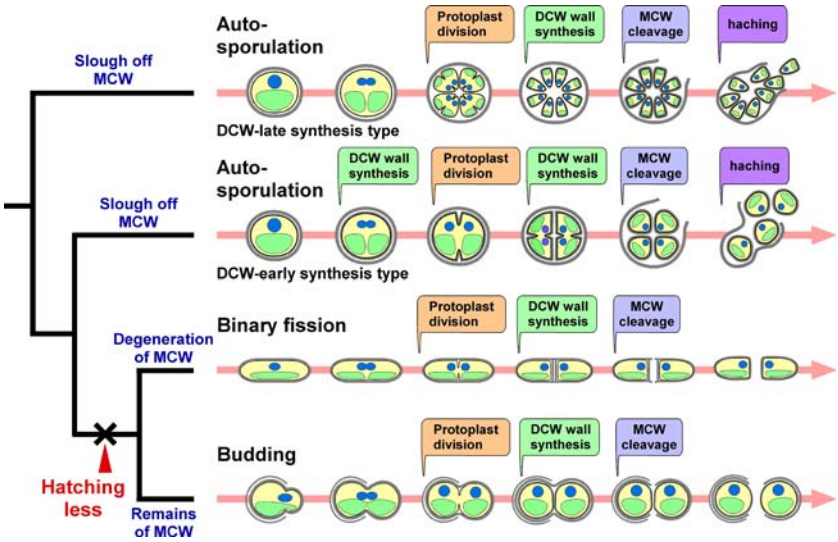

Fig. 19 Evolution of binary fission and budding from autosporulation. This scheme summarizes the timing of mother cell wall (*MCW*) cleavage and daughter cell wall (*DCW*) formation in three modes of cell division: autosporulation (modified from Yamamoto et al. 2004, 2005), binary fission, and budding. The divergence of early type daughter cell wall synthesis in autosporulation, late-type daughter cell wall synthesis in autosporulation, binary fission, and budding is indicated according to the topography of the phylogenetic tree based on actin sequences (*left*). A lack of shedding of the mother cell wall may have led to the development of binary fission and budding

plane of division (Fig. 16h, j). Similarly, in *M. geminata*, invagination of the plasma membrane alone was observed at the plane of division during budding (data not shown). These results suggest that binary fission and budding share a common ancestral non-hatching mode of cell division of the daughter cell wall-late synthesis type. Many ellipsoidal species propagate by binary fission. There are other ellipsoidal trebouxiophyceaen genera; for example, *Stichococcus* (Pickett-Heaps 1974; Neustupa et al. 2007) and *Koliellopsis* (Lokhorst et al. 2004), in which the cells unite to form filaments. In non-hatching *N. bacillaris*, if cleavage of the mother cell wall or separation of the daughter cells does not occur, the cells will join together to form filaments. The parallel emergence of multicellular algal species may have begun from processes such as filament formation.

Acknowledgments We thank Professors K. Ueda and T. Noguchi of Nara Women's University for providing *N. bacillaris*. We are grateful to Prof. M. Tsuzuki at the Tokyo University of Pharmacy and Life Sciences and Dr. A. Hirata at the University of Tokyo for helpful discussions. This work was supported in part by grants from the Kurita Water and Environment Foundation (S. K.), BRAIN (S. K.), a Grant-in-Aid for JSPS research fellows (M. Y.), a Grant-in-Aid from Senshu University in 2007, a Grant-in Aid from the Institute of Natural Sciences at Senshu University (M. Y.), and a Grant-in-Aid from the Nippon Life Insurance Foundation (M. Y.).

References

Arai S, Takahashi H, Takano H, Sakai A, Kawano S (1998) Isolation, characterization, and chromosome mapping of an actin gene from the primitive green alga, *Nannochloris bacillaris* (Chlorophyceae). J Phycol 34:477–485

Baba M, Osumi M (1987) Transmission and scanning electron microscopic examination of intracellular organelles in freeze-substituted *Kloeckera* and *Saccharomyces cerevisiae* yeast cells. J Electron Microsc 5:249–261

Belliveau DJ, Garbary DJ, McLachlan JL (1990) Effects of fluorescent brighteners on growth and morphology of the red alga *Antithamnion kylinii*. Stain Technol 65:303–311

Bhattacharya D, Stickel SK, Sogin ML (1991) Molecular phylogenetic analysis of actin genic regions from *Achlya bisexualis* (Oomycota) and *Costaria costata* (Chromophyta). J Mol Evol 33:525–536

Chida Y, Ueda K (1991) Division of chloroplast in a green alga, *Trebouxia potteri*. Ann Bot 67:435–442

Friedl T (1995) Inferring taxonomic positions and testing genus level assignment in coccoid green lichen algae: a phylogenetic analysis of 18S ribosomal RNA sequences from *Dictyochloropsis reticulata* and from members of the genus *Myrmecia* (Chlorophyta, Trebouxiophyceae cl. nov.). J Phycol 31:632–639

Henley WJ, Hironaka JL, Guillou L, Buchheim MA, Buchheim JA, Fawley MW, Fawley KP (2004) Phylogenetic analysis of the '*Nannochloris*-like' algae and diagnosis of *Picochlorum oklahomensis* gen. et sp. nov. (Trebouxiophyceae, Chlorophyta). Phycologia 40:641–652

Hindák F (1976) *Marvania geminata gen. nov. et sp. nov.*, a new green alga. Arch Hydrobiol 16(Suppl 49):261–270

Lokhorst GM, Star W, Zuccarello G (2004) New genus *Koliellopsis* (Trebouxiophyceae, Chlorophyta): its phylogenetic position inferred from ultrastructure and nuclear ribosomal DNA sequences. Phycol Res 52:235–243

McIntosh K, Pickett-Heaps JD, Gunning BES (1995) Cytokinesis in *Spirogyra*: integration of cleavage and cell-plate formation. Int J Plant Sci 156:1–8

Naumann E (1921) Notizen zur Systematik der Süßwasseralgen V. Über *Nannochloris*, eine neue Chlorophyceengattung. Ark Bot 16:1–19

Neustupa J, Šejnohová L (2003) *Marvania aerophytica* sp. nov., a new subaerial tropical green alga. Biologia 58:503–507

Neustupa J, Eliáš M, Šejnohová L (2007) A taxonomic study of two *Stichococcus* species (Trebouxiophyceae, Chlorophyta) with a starch-enveloped pyrenoid. Nova Hedwigia 84:51–63

Ogawa S, Ueda K, Noguchi T (1995) Division apparatus of the chloroplast in *Nannochloris bacillaris* (Chlorophyta). J Phycol 31:132–137

Pickett-Heaps JD (1974) Cell division in *Stichococcus*. Br Phycol J 9:63–73

Posada D, Crandall KA (1998) Modeltest: testing the model of DNA substitution. Bioinformatics 14:817–818

Sluiman HJ, Reymond OL (1987) Cell division in the green microalga *Marvania geminata*: semi-exogenous autosporogenesis, role of coated pit–microtubule complexes, and systematic significance. Acta Bot Neerl 36:231–245

Spurr AR (1969) A low-viscosity epoxy resin embedding medium for electron microscopy. J Ultrastruct Res 26:31–42

Swofford DL (2002) PAUP*: phylogenetic analysis using parsimony (and other methods). Beta version 10. Sinauer, Sunderland, MA, USA

Tschermak-Woess E (1999) Life cycle and supplementary comments on the light microscopic morphology of *Nannochloris eucaryota*. Plant Biol 1:214–218

Yamamoto M, Nozaki H, Kawano S (2001) Evolutionary relationships among multiple modes of cell division in the genus *Nannochloris* (Chlorophyta) revealed by genome size, actin gene multiplicity, and phylogeny. J Phycol 37:106–120

Yamamoto M, Nozaki H, Miyazawa Y, Koide T, Kawano S (2003) Relationships between presence of a mother cell wall and speciation in the unicellular micro alga *Nannochloris* (Chlorophyta). J Phycol 39:172–284

Yamamoto M, Fujishita M, Hirata A, Kawano S (2004) Regeneration and maturation of daughter cell walls in the autospore-forming green alga *Chlorella vulgaris* (Chlorophyta, Trebouxiophyceae). J Plant Res 117:257–264

Yamamoto M, Kurihara I, Kawano S (2005) Late type of daughter cell wall synthesis in one of the Chlorellaceae, *Parachlorella kessleri* (Chlorophyta, Trebouxiophyceae). Planta 221:766–775

Yamazaki T, Yamamoto M, Sakamoto W, Kawano S (2005) Isolation and molecular characterization of rbcS in the unicellular green alga *Nannochloris bacillaris* (Chlorophyta, Trebouxiophyceae). Phycol Res 53:67–76